The Cryosphere

Open Access

Event-driven deposition of snow on the Antarctic Plateau: analyzing field measurements with SNOWPACK

C. D. Groot Zwaaftink[1,4], A. Cagnati[2], A. Crepaz[2], C. Fierz[1], G. Macelloni[3], M. Valt[2], and M. Lehning[1,4]

[1]WSL Institute for Snow and Avalanche Research SLF, Davos, Switzerland
[2]ARPAV CVA, Arabba di Livinallongo, Italy
[3]Institute of Applied Physics – IFAC-CNR, Florence, Italy
[4]CRYOS, School of Architecture, Civil and Environmental Engineering, EPFL, Lausanne, Switzerland

Correspondence to: C. D. Groot Zwaaftink (groot@slf.ch)

Abstract. Antarctic surface snow has been studied by means of continuous measurements and observations over a period of 3 yr at Dome C. Snow observations include solid deposits in form of precipitation, diamond dust, or hoar, snow temperatures at several depths, records of deposition and erosion on the surface, and snow profiles. Together with meteorological data from automatic weather stations, this forms a unique dataset of snow conditions on the Antarctic Plateau. Large differences in snow amounts and density exist between solid deposits measured 1 m above the surface and deposition at the surface. We used the snow-cover model SNOWPACK to simulate the snow-cover evolution for different deposition parameterizations. The main adaptation of the model described here is a new event-driven deposition scheme. The scheme assumes that snow is added to the snow cover permanently only during periods of strong winds. This assumption followed from the comparison between observations of solid deposits and daily records of changes in snow height: solid deposits could be observed on tables 1 m above the surface on 94 out of 235 days (40 %) while deposition at the surface occurred on 59 days (25 %) during the same period, but both happened concurrently on 33 days (14 %) only. This confirms that precipitation is not necessarily the driving force behind non-temporary snow height changes. A comparison of simulated snow height to stake farm measurements over 3 yr showed that we underestimate the total accumulation by at least 33 %, when the total snow deposition is constrained by the measurements of solid deposits on tables 1 m above the surface. During shorter time periods, however, we may miss over 50 % of the deposited mass. This suggests that the solid deposits measured above the surface and used to drive the model, even though comparable to ECMWF forecasts in its total magnitude, should be seen as a lower boundary. As a result of the new deposition mechanism, we found a good agreement between model results and measurements of snow temperatures and recorded snow profiles. In spite of the underestimated deposition, the results thus suggest that we can obtain quite realistic simulations of the Antarctic snow cover by the introduction of event-driven snow deposition.

1 Introduction

The upper meter of the snow cover on the Antarctic Plateau is exposed to extreme conditions that influence the development of the snow cover. At Dome C, the annual mean temperature is $-53\,°C$, the annual mean wind speed is $2.9\,m\,s^{-1}$ (King and Turner, 1997), while the mean annual accumulation is less than about $40\,kg\,m^{-2}\,a^{-1}$ (for example, Petit et al., 1982; Frezzotti et al., 2005). Snow is transported by the wind before it is permanently added to the underlying snow cover. The snow cover at Dome C is therefore highly influenced by the wind (for example, Palais et al., 1982). A lot of effort has gone into describing the effect of the wind on the surface mass balance and the snow microstructure and stratigraphy (for example, Brun et al., 2011). To model the snow cover, however, we particularly need quantitative descriptions.

The effects of blowing snow on the snow cover are most easily visible in the surface features they form, such as dunes

and zastrugi. Watanabe (1978) describes the characteristics of surface features formed by wind and drifting snow, for example dunes, and the deposition-erosion processes at Mizuho Plateau. Doumani (1967) reports in detail on the formation of zastrugi and other erosional and depositional features. Another description of snow accumulation and the occurrence of dunes and zastrugi in a katabatic wind zone is given by Goodwin (1990). Although these observations are very valuable, we lack a quantitative description and especially observations of the wind and the properties of the snow while transported. More recently, Walden et al. (2003) collected ice crystals from precipitation and deposited snow on an elevated platform on the roof of a building at South Pole Station; however, they do not describe the snow surface.

More quantitative descriptions of Antarctic surface snow are found in the following studies. During a traverse between Syowa Station and the South Pole, surface density was measured at several stakes and was never found to be less than $210 \, kg \, m^{-3}$ (Fujiwara and Endo, 1971). Palais et al. (1982) made several 3 m snow profiles at Dome C and found a strong stratigraphic layering. Besides visible stratigraphy, gross β-radioactivity and microparticles were used to date the layers. However, snow properties such as density, grain and bond size or snow-cover temperatures were not measured. Gay et al. (2002) observed grain sizes at several locations in the Antarctic. They conclude that grain size is spatially homogeneous near the surface (0–0.5 m depth) and may be classified as very fine to fine ($< 0.5 \, mm$; see Fierz et al., 2009). Furthermore, they report that within one meter from the surface, the grain size at Dome C remains fine. Measurements of snow density within the top meter of the snow cover were performed during a recent Japanese–Swedish traverse (Sugiyama et al., 2012). These authors report nearly constant density values from Dome F (3800 m a.s.l.) to Kohnen (2890 m a.s.l.), ranging from 333 to $375 \, kg \, m^{-3}$ and averaging to $351 \, kg \, m^{-3}$. These observations however, describe the snow cover at a given time and do not give us information on the evolution of the Antarctic surface snow. A study by Radok and Lile (1977) provides surface snow density measurements over one year, during which time the minimum (monthly mean) surface density was $279 \, kg \, m^{-3}$. Birnbaum et al. (2010) combine qualitative and quantitative observations of dune formation at Kohnen station. According to their observations dune formation would only occur after days on which large amounts of loose heavy particles were generated at the surface by drifting snow. They also report that the dunes are of much higher density than the surrounding snow and that they typically consist of rounded particles. The observations cover three dune formation events in one austral summer.

Drifting snow processes are not only important for the surface snow characteristics; they also have an influence on the surface mass balance or accumulation. Several studies indicate that local erosion can be on the same order of magnitude as annual precipitation (for example, Petit et al., 1982).

This, combined with a lack of seasonal melting layers, makes it difficult to date snow layers in snow profiles and to understand total accumulation. Despite this, many efforts have been made to estimate the surface mass balance. For example, Frezzotti et al. (2007) estimated snow accumulation from ice core drillings and stake measurements. They found that accuracy is poor for low-accumulation sites.

While accumulation is already hard to measure, it may be even more difficult to distinguish between drifting snow and actual snowfall. Visual observations of the South Pole Weather Office distinguish diamond dust, blowing snow and snow grains. Often, however, blowing snow and diamond dust occur together (Walden et al., 2003). Furthermore, gauge measurements are problematic since drifting snow is blown into the gauges (Bromwich, 1988) and the snowfall amounts in this region do not exceed the minimum gauge resolution (Cullather et al., 1998). Combination of these facts decreases the accuracy of precipitation measurements and the estimations of the surface mass balance. This problem could be overcome, however, by continuously recording precipitation, height of snow and surface snow characteristics such as density and snow type as discussed in this paper.

Several authors already modelled the Antarctic snow cover. Morris et al. (1997) used DAISY, a physics-based snow model, to simulate the snow cover at Halley Bay. Initial new snow density was set to 300 or $400 \, kg \, m^{-3}$ in different simulations. Dang et al. (1997) used a similar approach with the snow-cover model CROCUS, setting the initial new snow density to either 300 or $350 \, kg \, m^{-3}$. In a further study with CROCUS, Brun et al. (1997) proposed to account for new snow densification in cold and windy conditions. Vionnet et al. (2012) describe this approach in detail that combines surface snow characteristics and threshold wind speeds, that is, drifting and blowing snow conditions, to attain an effective compaction of surface snow down to about 10 cm below the surface. In this way, compaction due to wind may still occur days or weeks after deposition. Recently, Brun et al. (2011) modelled the snow cover at Dome C for 10 days in January 2010. The aim was to show that in this region a snow-cover model can be coupled successfully to an atmospheric model as long as the surface energy balance is correctly reproduced. However, over such a short period of time the authors did not have to consider either settlement or accumulation and the model reproduces snow temperatures quite well from the surface down to about 80 cm depth. In addition, Gallée et al. (2001) have shown how relevant an accurate representation of surface snow properties is for both drifting snow and surface mass balance modelling.

We use the snow-cover model SNOWPACK that has been extensively tested for Alpine regions (for example, Lehning and Fierz, 2008; Fierz and Lehning, 2001), but has not been previously applied in Antarctica. Since we look at timescales of several years it is necessary to drive the model with accurate precipitation amounts. As described above, measurements or estimations of precipitation in Antarctica are not

straightforward. Furthermore, we know from the mentioned studies and our own observations that wind plays a key role eroding and depositing snow at the surface. But how can we represent this in a one-dimensional snow-cover model? We suggest not to use the precipitation directly, but to add snow to the modelled snow cover during events of drifting snow, hypothesizing that deposition is associated with periods of strong wind rather than with precipitation. A further issue within that context is the density of the "new" snow added to the underlying snow cover. Our observations at Dome C show that the bulk density of snowfall is quite often lower than $60 \, \mathrm{kg \, m^{-3}}$, in contrast to the surface snow density mentioned above. The large difference in density of solid deposits and the surface snow density can be ascribed to the wind. A few theories of the mechanisms behind this densification have been suggested, (for example, Seligman, 1936; Pomeroy and Gray, 1995). First of all, during drifting snow events, snow particles become smaller due to collisions and enhanced sublimation. These effects have been frequently observed, but not often quantified (Sato et al., 2008). The smaller particles may then pack closer together or fill gaps between unaffected, larger ones that are already immobilized, increasing the density. Another theory considers the humidity. In drifting snow, the air is close to saturation. Some authors, (for example, Kotlyakov, 1966), indicate that this enhances the density because fast sintering may be facilitated. However, in the snow cover, the air is close to saturation too and it is questionable whether supersaturation will have such a strong effect, especially at these low snow temperatures. This is underlined by the generally small latent heat flux at the surface.

Below we will present a three-year study of the snow cover at Dome C that includes meteorological observations, erosion studies, snow profiles, and numerical simulations. We start with a description of our data set in Sect. 2. In Sect. 3 we briefly describe the adaptation of the model SNOWPACK to polar conditions. In particular, a new parameterization for event-driven deposition is introduced. We attempt to model the rapid densification of surface snow by a suitable parameterization depending on mean wind speed over a given period. We will thus account for some general effect of the wind on the snow properties, but will not try to fully explain the physical processes behind the densification found at the surface. Furthermore, care is taken to obtain realistic settling rates of the underlying snow cover. In Sect. 4 we then discuss our results by comparing simulation output with measurements like snow heights recorded at stake farms, emitted longwave radiation, continuous records of snow temperatures, and observed snow profiles.

2 Data

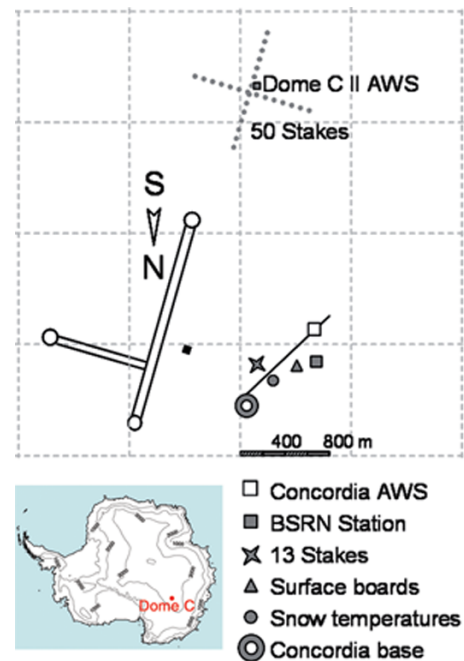Concordia research station (75°06′ S, 123°24′ E, 3233 m a.s.l.) is located at Dome C on the Antarctic

Fig. 1. Top: plan of the immediate surroundings of Concordia research station indicating all measurement sites. The measurement site "Surface boards" includes the surface boards $\mathrm{SB_{acc}}$ and $\mathrm{SB_{clear}}$ and the tables used for measurements of solid deposits. Bottom: map of Antarctica indicating Dome C.

Plateau. The station is mainly used for research studies in geodesy, glaciology, human biology, seismology, astronomy, and for meteorological and geomagnetic observations as well as for environmental monitoring. Near the base there are two Automatic Weather Stations (AWS), that is, Dome C II and Concordia AWS, and a station of the Baseline Surface Radiation Network (BSRN Station) (see Fig. 1). Other sites are dedicated to snow temperature measurements or to observations of both solid deposits (tables above the surface) and drifting snow (snow boards lying on the surface, indicated as surface boards in Fig. 1). In addition, accumulation is measured at two stake farms. According to our observations between January 2005 and December 2009, extremely low air and snow surface temperatures (−81 to −12 °C and −80 to −19 °C, respectively), and generally low wind-speed conditions (5-yr mean $3.1 \, \mathrm{m \, s^{-1}}$, maximum hourly mean $16.2 \, \mathrm{m \, s^{-1}}$) are recorded at Dome C. Under anti-cyclonic flow prevailing winds come from the SSW direction (Genthon et al., 2010). Below we will only describe measurements of interest to our study, covering the period from January 2005 through July 2009.

2.1 Meteorological records

Continuously recorded meteorological data next to Concordia research station at Dome C include air temperature and relative humidity, incoming shortwave and longwave

radiation, and wind speed and direction. Air temperature and relative humidity were measured at 2 m height with a platinum resistance thermometer at Dome C II and a HUMICAP® at Concordia AWS, respectively. Wind speed and direction were taken from Dome C II, where a mechanic Young sensor is located at a height of about 3 m above the surface. Incoming long and shortwave radiation measurements were taken from the Dome C BSRN station, which is equipped with two normal incidence Kipp & Zonen CM21 pyranometers and a Kipp & Zonen CG4 Pyrgeometer, all operated according to BSRN guidelines (Lanconelli et al., 2011). In addition, the Institute of Atmospheric Sciences and Climate of the Italian National Research Council (ISAC/CNR, V. Vitale) provided measurements of upwelling longwave and reflected shortwave radiation. All measurements were recorded at different time steps and intervals but we use hourly averages to drive the snow-cover model. Whenever necessary, data gaps were filled by interpolation.

2.2 Solid deposits, snow deposition, and erosion

Four methods of observing solid deposits as well as deposition and erosion at Dome C provided data discussed in the current study. Figure 1 shows the location of the different measurement sites. By solid deposits we refer to precipitation (snowfall), diamond dust and hoar. These have the potential to be added to the snow cover. With deposition and erosion we refer to the changes in snow height, or the actual effects on the surface of the snow cover, mainly induced by the wind.

We simultaneously measured the depth and the density of solid deposits on wooden tables 1 m above the surface. Edges 5 cm in height on 3 sides of the tables helped protect the deposits from being blown away by the wind. The density was measured through weighing. When there was too little snow deposit for a reliable weight measurement, we estimated density based on the snow crystal forms. For this purpose typical densities were inferred from our set of measured data, from $44 \, \mathrm{kg \, m^{-3}}$ for needles (PPnd) to $107 \, \mathrm{kg \, m^{-3}}$ for small rounded particles (RGsr; for the abbreviations, see Fierz et al., 2009).

Furthermore, two stake farms allow accumulation on a larger scale around Dome C to be assessed. The first farm, located about 500 m away from the base but close to Concordia AWS, consists of 13 stakes arranged in two 60 m lines forming a cross. At this location observations were made weekly from January 2006 to March 2009. The other field, located about 3 km away from the base, next to Dome C II, includes 50 stakes placed 25 m apart from each other, also arranged in a cross (see Fig. 1). Due to the distance of the latter field from the base, those snow height measurements are only available on a monthly basis during the summer seasons of 2005 to 2008.

The two last methods focus on the erosion and deposition of snow on the snow cover and involve measuring snow height on two snow boards (SB_{clear} and SB_{acc}) placed flush with the snow surface. To assess deposition at the surface, snow board SB_{clear} is cleared daily and set level again with the surface while snowboard SB_{acc} is not. Thus SB_{clear} yields the daily deposition and SB_{acc} gives the cumulated height of snow due to both deposition and erosion. Observations of erosion and deposition events at the surface are available over the period from November 2008 through June 2009.

2.3 Snow temperatures

Snow temperatures were monitored continuously by means of two strings of resistance temperature detectors (RTD, PT 100 DIN-A) placed into the snow cover at initial depths of 5, 10, 50, and 100 cm (at a location 3 to 4 m away from a shelter) and 150, 200, 250, 300, 400, 500, 600, 800, and 1000 cm (at 5 to 7 m from the same shelter). Surface disturbances due to drifting and blowing snow around the shelter are known to occur but were not recorded. The upper four sensors were reinstalled in February 2006, February 2008, and December 2008 to minimize the effect of settlement and accumulation on their position relative to the surface.

2.4 Snow profiles

Several snow profiles were taken in the summers between December 2004 and December 2008. Snow profiles are records of the stratigraphy of the snow cover. Density, grain shape and size, temperature and hand hardness are usually observed layer by layer on the wall of an open pit. Most snow pits were about 1 m deep, but occasionally deeper pits were dug. In addition, we took 16 series of 8 density measurements each of the top 10 cm of the snow cover over a 12 months period.

We combined several profiles taken at different locations around Dome C from December 2004 to January 2005 as well as measurements from a shallow core to build an approximately 10-m deep initial profile for our simulations.

3 The snow-cover model SNOWPACK: adaptation to the Antarctic Plateau environment

SNOWPACK is a one-dimensional physical snow-cover model. Driven by standard meteorological observations, the model describes the stratigraphy, snow microstructure, snow metamorphism, temperature distribution, and settlement as well as surface energy exchange and mass balance of a seasonal snow cover. It has been extensively described in Lehning et al. (2002a, b) and Lehning and Fierz (2008). In this section we focus on the adaptations made to make the basic model (release 3.0.0) suitable for the Antarctic Plateau environment.

3.1 Event-driven snow deposition

Single strong wind events at Dome C have a large impact on snow properties and can erode more snow than the yearly precipitation (for example, Petit et al., 1982). We incorporate the effect of drifting snow events in our simulations by introducing event-driven deposition. This is based on the assumption that longer periods of drifting snow alter the snow surface significantly and snow can only become immobile through densification during strong drifting snow events, as discussed in the introduction. Observations of dune formation from eroded snow as described by Birnbaum et al. (2010) and our observations of deposition and erosion combined with measurements of both wind and solid deposits (at 1 m) support this assumption. We furthermore assume that both erosion and deposition occur locally. While it is clear that precipitation will partly contribute to long-term accumulation, local and time-accurate accumulation can only be estimated if the deposition and erosion dynamics are considered.

To estimate the wind speed needed for an event to occur, we compared the snow height measurements on the boards placed on the snow surface (see Sect. 2.2) with the wind speed records. We chose to look at the 100-h average wind speed, as observers indicate that strong erosion and deposition events occur during storms of several days. Based on these two observations, a 100-h average wind speed of at least $4 \, \mathrm{m \, s^{-1}}$ is required to eventually add snow to the underlying snow cover. This wind speed limit is well below an often assumed drifting snow threshold of $7 \, \mathrm{m \, s^{-1}}$ at 10 m above the surface (for example, Pomeroy et al., 1993; Clifton et al., 2006), corresponding to about $6 \, \mathrm{m \, s^{-1}}$ at 3 m above the surface (assuming a logarithmic wind profile with a roughness length of 1 mm). However, whereas the initiation of drifting snow may require high wind speeds, maintaining it does not (for example, Mellor, 1965). More importantly, a 100-h average wind speed of $4 \, \mathrm{m \, s^{-1}}$ implies high wind speeds during shorter periods and therefore includes the gusts that could easily initiate drifting snow. In summary, we assume an event to occur whenever the 100-h moving average of the wind speed measured at 3 m height, U_{event}, exceeds $4 \, \mathrm{m \, s^{-1}}$. During our total observation period, U_{event} exceeded $4 \, \mathrm{m \, s^{-1}}$ about 23 % of the time. We only add snow to the snow cover in case of such an event: all solid deposits measured since the last event is summed up and added to the modelled snow cover once a new event takes place.

As discussed in the introduction, the wind densifies new snow (see also Fig. 2), probably mainly through rounding and decreasing the size of the particles. Since we only add snow that has been transported by the wind, we need to account for this effect in the initial density of snow added to the snow cover. We neither have measurements that allow us to formulate a precise dependency of snow density on wind speed nor can we describe this process physically. Therefore we looked for a simple relation to obtain an initial snow den-
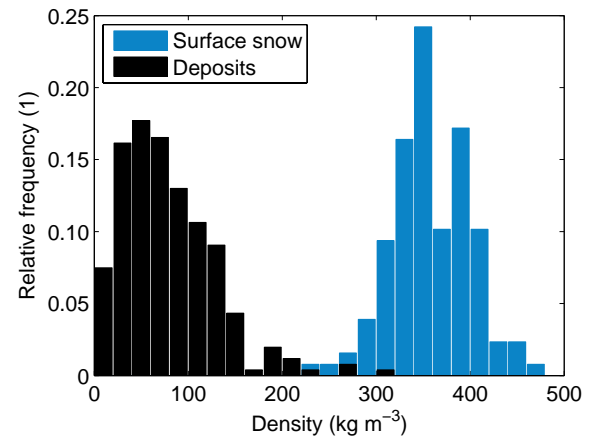

Fig. 2. Relative frequency distribution of the measured density of solid deposits (254 measurements, March 2005–March 2009) and surface snow down to a depth of 10 cm (128 measurements, May 2008–March 2009).

sity. We use a logarithmic dependency on the wind speed as we expect that there will be an upper limit on densification through snow transport. The density ρ_{n} of the "new" surface snow added to the snow cover, for values of U_{event} between 4 and $7 \, \mathrm{m \, s^{-1}}$, is thus estimated according to

$$\rho_{\mathrm{n}} = 361 \cdot \log_{10}\left(\frac{U_{\mathrm{event}}}{U_0}\right) + 250, \qquad (1)$$

where $U_0 = 4 \, \mathrm{m \, s^{-1}}$ Over the range of 250 to $340 \, \mathrm{kg \, m^{-3}}$, density thereby increases by about $30 \, \mathrm{kg \, m^{-3}}$ for an increase in wind speed of $1 \, \mathrm{m \, s^{-1}}$. The coefficients in Eq. (1) are such that (a) the minimum density corresponds to minimum values observed in our and other studies mentioned in the introduction and (b) after a simulation period of about 10 yr, the snow reaches a mean density in the upper 10 cm of about $320 \, \mathrm{kg \, m^{-3}}$. The impact of using Eq. (1) will be discussed further in Sect. 4.2.

Not only density, but also the microstructure parameters of newly added snow are adapted to drifting snow conditions: dendricity and sphericity are initially set to 0.5 and 0.75, respectively, or to 0.15 and 1 if the mean hourly wind speed exceeds $5 \, \mathrm{m \, s^{-1}}$. In addition, whenever the 100-h moving average of relative humidity of the air with respect to ice is greater than 75 %, we assume increased bond growth, leading to a larger bond size. The introduction of events to add snow gives the modelled permanent snow cover a pronounced stratigraphy with fewer single layers since snowfall is collected between two deposition events (see Sect. 4.5).

3.2 Surface compaction by wind

The overburden pressure on surface snow is minimal and will therefore produce little compaction. Low temperatures will not promote a rapid settlement due to metamorphic processes either. However, as Brun et al. (1997) pointed out, wind may

further compact surface snow and they used that effect to render simulations of polar snow more realistic. SNOWPACK also features such a compaction mechanism that enhances the basic strain rate, $\dot{\varepsilon}$, down to a depth of 0.07 m below the snow surface according to

$$
\begin{aligned}
\dot{\varepsilon}_{\text{enh}} &= (1 + g(u))\,\dot{\varepsilon}, \\
g(u) &= \begin{cases} A_{\text{enh}}(d)(u - u_0)^n, & u > u_0 \ , \\ 0 \end{cases}
\end{aligned}
\tag{2}
$$

where u is the mean hourly wind speed (m s^{-1}), u_0 is a threshold velocity ($5\,\text{m s}^{-1}$) and $A_{\text{enh}}(d)$ is a function of depth, d (m), below the snow surface. In the basic version of SNOWPACK, $n = 1$ and $A_{\text{enh}}(d)$ is a constant set to $A_{\text{enh},0} = 5\,\text{s m}^{-1}$. This proves to be quite inefficient if the surface snow has already reached a density of more than $250\,\text{kg m}^{-3}$. Thus, in this study, we run simulations with $n = 3$ and the following depth dependence for $A_{\text{enh}}(d)$:

$$
A_{\text{enh}}(d) = 2.7 A_{\text{enh},0} \left(1 - \frac{d}{1.25\,d_{\text{max}}} \right),
\tag{3}
$$

that is, the effect decreases linearly with depth to reach 20 % of its surface strength at the deepest affected depth d_{max} (0.07 m). Unfortunately, there are no data available to test these model implementations; they simply represent a conceivable additional compaction process for surface snow based on current knowledge of drifting and blowing snow. For example, the exponent $n = 3$ is taken from the well known dependency of drifting snow mass flux on wind speed (see, for example, Nishimura and Hunt, 2000).

3.3 Snow settlement

Snow temperatures at Dome C hardly ever rise above $-20\,°\text{C}$ and the temperature dependence of the snow viscosity, $\eta(T_s)$, dominates the snow settlement process:

$$
\dot{\varepsilon} = \sigma \big/ \eta(T_s),
\tag{4}
$$

where σ is the overburden stress. Below we describe a new temperature dependence of snow viscosity that has recently been introduced in SNOWPACK. It covers the temperature range from -80 to $0\,°\text{C}$. Parameterizations of the Arrhenius-type are often used to describe the temperature dependence of mechanical properties of snow. However, to avoid a barely compressible snow cover at temperatures below roughly $-50\,°\text{C}$, the activation energy Q must be compatible with the material snow. Schweizer et al. (2004) measured snow toughness from $-20\,°\text{C}$ near to the melting point and their results suggest a value of $16\,080\,\text{J mol}^{-1}$ for Q compared to $67\,000\,\text{J mol}^{-1}$ for ice. The same authors also showed that toughness drastically decreases for temperatures above roughly $-8\,°\text{C}$, eventually reaching zero at the melting point. We take account of this fact by multiplying the Arrhenius term by a power law as is often done to describe

critical phenomena near a phase transition. This results in the following relation:

$$
\eta(T_s) \propto f(T_s) = \exp\left(-\frac{Q_s}{R}\left(\frac{1}{T_{\text{ref}}} - \frac{1}{T_s} \right) \right)
$$
$$
\left(0.3(T_m - T_s)^\beta + 0.4 \right),
\tag{5}
$$

where T_s (K) is the snow temperature, T_{ref} the threshold temperature discussed above (265.15 K), T_m the melting point of ice (273.15 K), R the gas constant ($8.31\,\text{J mol}^{-1}\,\text{K}^{-1}$), β the critical exponent (0.7), and Q_s the activation energy of snow. From our calibrations with Alpine snow it turns out that a value of $26\,130\,\text{J mol}^{-1}$ works best throughout the full temperature range of interest. This value is higher than suggested by Schweizer et al. (2004), which may be due to the different temperature ranges considered in their and our study. In Fig. 3 we compare Eq. (5) to both the previously implemented temperature term

$$
f_{\text{old}}(T_s) = 9.0 - 8.7 \exp(0.015(T_s - 273.15)),
\tag{6}
$$

and a pure Arrhenius term taking for Q_s the ice value and 263 K for T_{ref} as in the original formulation (Lehning et al., 2002a). It appears clearly that at temperatures below roughly 245 K, $f(T_s)$ increases much less than the pure Arrhenius law for ice while being about 50 times larger than $f_{\text{old}}(T_s)$ at 200 K. Thus the new temperature dependence of viscosity results in stiffer snow at low temperatures. Nearing the melting point, however, $f(T_s)$ shows a more pronounced temperature dependence than both the other parameterizations (see insert in Fig. 3). In other words, snow will still settle a little at low temperatures while maintaining the properties of seasonal snow as temperature is nearing the melting point.

3.4 Snow albedo

The current multi-linear regression for snow albedo used in SNOWPACK is similar to the one proposed in Lehning et al. (2002b):

$$
\alpha = \alpha_0 + \ln \left(1.442 + \sum_{i=1}^{12} a_i\,Q_i \right).
\tag{7}
$$

Table 1 summarizes the terms and coefficients of Eq. (7). For the Antarctic application, however, we applied the following changes to the standard parameterization: we dropped the age term $a_1 Q_1$ that describes accumulation of mineral dust and other "dark matter" at the surface. Based on a comparison with the albedo measured at the BSRN station, we reduced the value of α_0 from 0.8042 to 0.7542 to get the mean modelled albedo closer to measurements (see Sect. 4.4).

3.5 Initial and boundary conditions

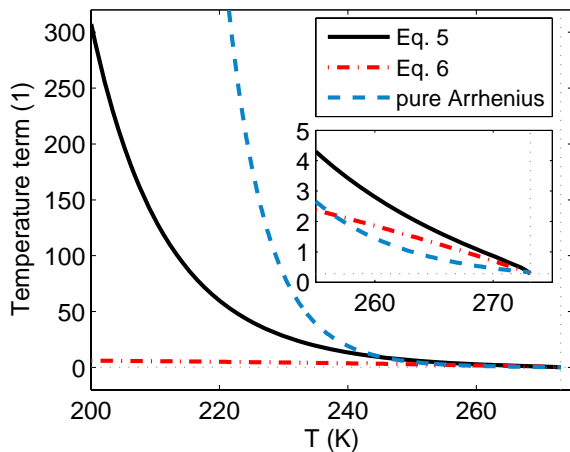We use Neumann boundary conditions at the surface of our model snow cover. Turbulent fluxes are computed using a

Fig. 3. Temperature term of the viscosity according to the current formulation (Eq. 5), the previous parameterization (Eq. 6) and a pure Arrhenius term as described in Sect. 3.3. The new temperature dependence of viscosity results in stiffer snow at low temperatures while nearing the melting point a more pronounced temperature dependence than both the other parameterizations is achieved (see insert).

Table 1. Description of the terms (Q_i) in Eq. (7). The coefficient values correspond to the standard SNOWPACK implementation (release 3.0.0).

Index	Coefficient	Description	Units
0	0.8042	Average albedo	1
1	−0.000575	Age of surface snow, limited to 30 days at most	d
2	0.00459	Snow surface temperature	K
3	−0.006	Air temperature	K
4	0.0333	Relative air humidity	1
5	0.00762	Wind speed	$\mathrm{m\,s^{-1}}$
6	−0.000101	Reflected shortwave radiation	$\mathrm{W\,m^{-2}}$
7	−0.000056	Snow density	$\mathrm{kg\,m^{-3}}$
8	−0.2735	Volumetric liquid water content	1
9	0.175	Grain size	mm
10	−0.301	Bond size	mm
11	0.064	Dendricity	1
12	−0.0736	Sphericity	1

Monin–Obukhov scheme considering stability corrections, as described by Stearns and Weidner (1993). The deepest available snow temperature record provides the lower Dirichlet boundary condition. The snow temperature of −54 ± 1 °C at this depth of 10 m roughly represents the mean annual air temperature at Dome C. We further assume that settlement is negligible over a few years at this depth.

Our initial snow profile was constructed from several snow profiles taken at several locations around Concordia research station. We then used the first simulation year (28 January 2005 to 15 February 2006) as a "spin-up time" for the different parts of this profile to adjust to each other regarding

deformation rate and snow temperature. At the end of this spin-up run, we adapted the temperatures within the top meter of the simulated snow profile to the values measured by the upper four temperature sensors that were relocated about 10 days earlier. This allows starting our main simulation with temperatures comparable to the measurements in the top meter of the snow cover while hardly affecting the temperature profile below this level. This profile then initializes our main simulation that runs through 1 March 2009.

In order to compare modelled and measured snow temperatures, we specially mark elements at those depths of our model snow cover that correspond to the location of temperature sensors on 15 February 2006. The marked depths of the upper four sensors were reassigned whenever these sensors were relocated. We further mark the first newly deposited element at the surface as a horizon to separate newly deposited snow from the old snow cover. Finally, we mark the element located at 5 m depth on 15 February 2006 to monitor settlement rate. All these marked elements then follow the settlement of the modelled snow cover.

4 Results and discussion

We first discuss the results of the experiment where deposition on the surface is compared to measurements of solid deposits above the surface, as this is the basis for our event-driven model approach. Then we validate the model by comparing modelled snow height changes to stake measurements, modelled to measured snow temperatures, and the modelled stratigraphy to snow profiles. We made several simulations to distinguish the effects of initial snow density, event-driven deposition, and additional surface compaction. All simulations are listed in Table 2. We will discuss particular simulations in detail and will briefly address the performance of the others where adequate.

4.1 Precipitation, deposition, and erosion

We start by comparing the estimated amount of daily precipitation with the 24-h ECMWF operational forecast for a $1.125° \times 1.125°$ grid. Not considering hoar deposition but including diamond dust, the observed solid deposits measured on tables 1 m above the surface represent the estimated daily precipitation. Forecasted and estimated amounts compare rather well from March to November 2006, especially regarding the cumulated sums over this period, 6.6 and $5.7\,\mathrm{kg\,m^{-2}}$, respectively. These results are encouraging with regard to validating numerical weather prediction in Antarctica with the method used here to measure solid deposits. However, the deposits collection method may be prone to significant error, which needs to be assessed in much more detail in the future. A larger data set including in particular more observations from the winter season is needed to confirm the above finding. We consider the measurement method

Table 2. All simulations performed to test the adaptations made to SNOWPACK. We define each simulation and summarize how snow density of new snow was initialized, if the snow was deposited at time of measurement or in events (Sect. 3.1) and if additional surface compaction (Sect. 3.2) was activated.

Name of simulation	Initial snow density (kg m^{-3})	Deposition during events	Surface compaction, Eqs. (2) and (3)
$\rho_{n, measured}$	Measured	No	No
$\rho_{n, measured} + SfcComp$	Measured	No	Yes
$\rho_{n, 250}$	250	No	No
$\rho_{n, 250} + SfcComp$	250	No	Yes
$\rho_{n, 250} + Event$	250	Yes	No
$\rho_{n, 250} + Event + SfcComp$	250	Yes	Yes
$\rho_{n, 320}$	320	No	No
$\rho_{n, 320} + SfcComp$	320	No	Yes
$\rho(U_{event})$	see Eq. (1)	Yes	No
$\rho(U_{event}) + SfcComp$	see Eq. (1)	Yes	Yes

to give a lower bound to the true precipitation as it is much more likely that precipitation particles either do not land on the table due to flow distortion or deposits are blown away from the table than that snow from the surface would additionally deposit on the table.

Next we compare the observed daily solid deposits (black solid bars in Fig. 4) with the observed daily "new" snow height on the surface (open bars in Fig. 4). As can be clearly seen in the upper panel of Fig. 4, the height of deposits on the table is usually less than measured on SB$_{clear}$, the daily cleared board flush with the snow surface. This is mainly due to the larger effect of drifting and blowing snow at the surface and Fig. 4 confirms that snow height changes at the surface and amounts of solid deposits 1 m above the surface are not necessarily linked. Comparing the density of the solid deposits to that of surface snow down to a depth of 10 cm further corroborates the above (see Fig. 2). The daily observations of solid deposits cover the entire study period and the mean density of over 200 measured deposits is 83 ± 43 kg m^{-3}, where the uncertainty here and henceforth refers to one standard deviation of the mean. On the other hand, all measurements of surface-snow density taken together averaged 357 ± 50 kg m^{-3}, covering the range from 234 to 460 kg m^{-3}, and the means of each series averaged 357 ± 14 kg m^{-3}. These results suggest a considerable spatial variability but a minimal change in mean surface snow density in time. These observations on surface snow agree well with observations at other high elevation locations in Antarctica as mentioned in the introduction.

The difference between the measurements on the two surface boards is interesting. The observations on both 20 and 21 November 2008 show that in total over one day, there was deposition on SB$_{clear}$ while snow was eroded from SB$_{acc}$, the accumulating board. This may indicate a large spatial heterogeneity of erosion and deposition. Although this would require transport perpendicular to the prevailing wind direc-
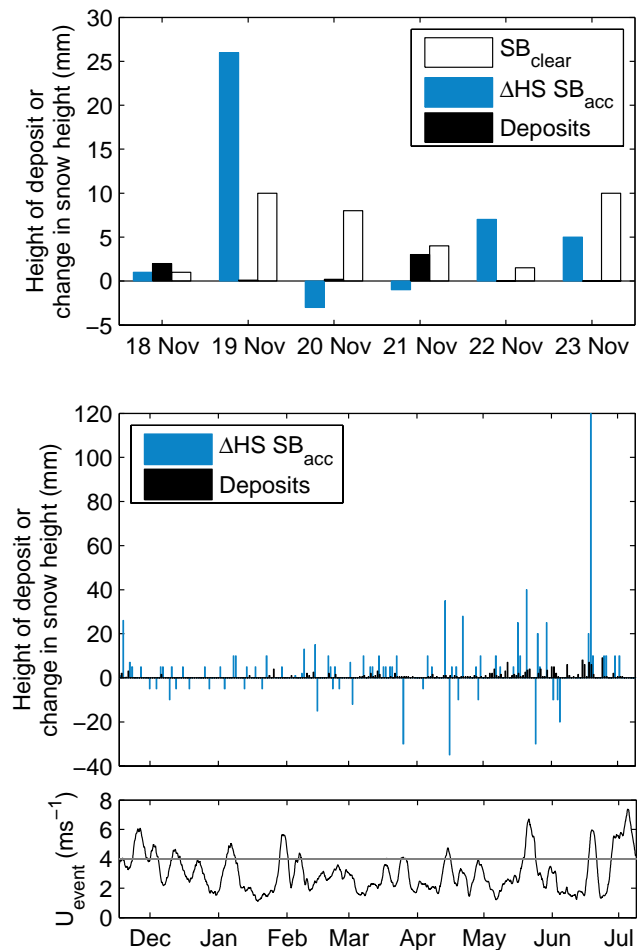

Fig. 4. Height of solid deposits (mm) measured daily either on a table 1 m above the surface or at the surface on a daily cleared snow board (SB$_{clear}$), and change of snow height ΔHS over an untouched snow board (SB$_{acc}$). Top: 18–23 November 2008; middle: 18 November 2008–July 2009, board SB$_{clear}$ not shown. Bottom: 100-h moving average wind speed (U_{event}, m s^{-1}) in black, 18 November 2008–July 2009. The grey line represents the minimum wind speed (4 m s^{-1}) necessary for an event (see Sect. 3.1).

tion, we cannot fully rule out transport between the adjacent boards. In the middle panel of Fig. 4 we therefore removed all cases where there was deposition on SB$_{clear}$ but erosion on SB$_{acc}$ to analyse the results over a longer period from 18 November 2008 to 3 July 2009. Here we focus on the change of snow height ΔHS on SB$_{acc}$ compared to the height of deposits measured on the table. Again, the heights of solid deposits measured on the table clearly do not match the snow height changes at the surface. The bottom panel shows the 100-h moving average of the wind speed and – in combination with the middle panel – points at an effect of the wind on deposition and erosion.

The daily solid deposits are very small and occur quite continuously, whereas the snow height changes are less frequent and generally larger. We frequently observed changes

at the surface on the order of 10 mm, corresponding to about 3.6 kg m^{-2} or 9.2 % of the mean yearly accumulation as inferred from stake measurements between 1996 and 1999 (39 ± 14 kg m^{-2} a^{-1}, Frezzotti et al., 2005). Our simulations should better represent this behaviour due to the introduction of events. But do we add the right amount of snow on a timescale of several months when we use the sum of solid deposits? Over this entire period of 7.5 months, the height of solid deposits on the table cumulated to 164.5 mm. Taking the mean deposit density of 83 kg m^{-3} mentioned in Sect. 2.2, this amounts to 13.7 kg m^{-2} or 35 % of the mean yearly accumulation. On 3 July 2009, snow height on SB$_{acc}$ amounted to 120 mm or 42.8 kg m^{-2} taking our measured mean surface density of 357 kg m^{-3}. Since some transport from SB$_{acc}$ to SB$_{clear}$ may have occurred, we regard this as the lower boundary of total deposition at the surface. The upper boundary can be obtained by summing up ΔHS over the full period. This yields 348 mm or 124.2 kg m^{-2}. We have to note that this measurement is done on a single location and may not be representative of the deposition at Dome C. Nonetheless, these measurements are an indication that on timescales of a few months we may strongly underestimate the amount of snow added to the snow cover when using measurements of solid deposits to drive SNOWPACK.

Summing up, both the sum of solid deposits and the snow mass deduced from snow height changes on a surface board differ substantially from the mean yearly accumulation. None of the measurements above thus seems to reliably represent the contribution from precipitation needed to drive snow-cover models. The solid deposits observed on the tables 1 m above the surface, however, are to a very large extent available daily throughout our entire simulation period of three years. This, and the fact that after subtracting the hoar deposition there is a good correspondence with cumulated forecast precipitation, led us taking them as is to drive SNOWPACK.

4.2 Stakes

To verify how the model performs during the complete period of simulation, we show in Fig. 5 the computed height of snow relative to the snow layer which was at the surface on 15 February 2006 and we compare it with snow-height changes recorded at the 13-stakes farm since the same date. The simulations named "$\rho_{n, measured}$" and "$\rho_{n, 320}$" both use the standard SNOWPACK set-up to add snow during snowfall periods, taking either the measured density of the snow deposit or a fixed initial density of 320 kg m^{-3}. This means that the model adds the observed water equivalent of a solid deposit to the underlying snow cover whenever the observation was made. In the "$\rho(U_{event})$" simulation, the model adds snow only at times of events as described in Sect. 3.1. "$\rho(U_{event})$ + SfcComp" applies in addition the surface compaction by wind described in Sect. 3.2. The total amount of solid deposits is the same in all four
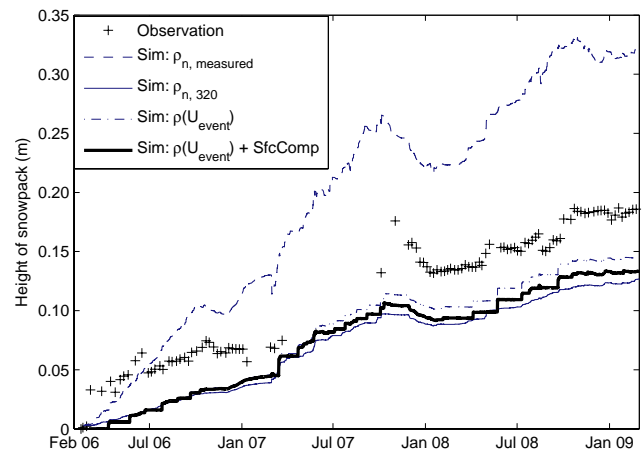

Fig. 5. Height of snowpack (m) relative to the snow layer which was at the surface on 15 February 2006. Stake measurements are indicated by crosses, and lines represent results from SNOWPACK simulations using as input either the measured density of solid deposits ("$\rho_{n, measured}$"), a fixed density of 320 kg m^{-3} ("$\rho_{n, 320}$"), both at precipitation time, or the event-driven mechanism without ("$\rho(U_{event})$") or with additional compaction due to wind at the surface ("$\rho(U_{event})$ + SfcComp").

simulations, that is, 42.4 kg m^{-2} over 36.5 months or about 14 kg m^{-2} a^{-1}. Both event-driven simulations, $\rho(U_{event})$ and $\rho(U_{event})$ + SfcComp, use the surface snow density given by Eq. (1), resulting on 10 December 2008 in a density of the top 10 cm of 266 and 291 kg m^{-3}, respectively.

In simulation "$\rho_{n, measured}$", SNOWPACK clearly overestimates the changes in snow height. This indicates that the measured or estimated density of the deposits is too low and therefore not representative of the snow added to the snow cover. The very low initial overburden and the prevailing low air and snow temperatures cannot overcome this shortcoming by either settlement or a metamorphic process. In the event-driven simulations "$\rho(U_{event})$" and "$\rho(U_{event})$ + SfcComp", snow height is increasing stepwise, unlike the simulation "$\rho_{n, 320}$" that adds snow at precipitation time with a fixed density of 320 kg m^{-3}. From the final difference of roughly 6 cm in measured to modelled snow height in run "$\rho_{n, 320}$", we infer that we may underestimate the deposited mass of snow despite the realistic snow density by at least 33 %, which is less than over shorter periods as discussed in Sect. 4.1.

Nevertheless, the sudden changes in snow height introduced by the events correspond qualitatively to the measured snow height and the model roughly catches the mean snow height increase, despite several drifting snow events leading to larger mismatches as in June 2006 and October 2007.

4.3 Settlement of the underlying snow cover

Even though the small overburden stress hardly contributes to the compaction of surface snow, settlement of the older,

underlying polar snow has to be as realistic as possible (see Sect. 3.3). Thus at initialization time we mark an element at 5 m depth and the surface element (see Sect. 3.5) and follow these throughout the simulation. That way we can compare the model results to either other models or measurements of snow settlement. Because models found in the literature also require fitting (see, for example, Arthern et al., 2010), we prefer to compare our results to measurements. However, as Arthern et al. (2010) point out, there are surprisingly few in situ observations of Antarctic snow compaction and, to our knowledge, none from Dome C. Their measurements of compaction for the 0 to 5 m depth range at Berkner Island yield a mean compaction rate of about $6.6 \times 10^{-10}\,\mathrm{s}^{-1}$. After three years of "$\rho(U_{\mathrm{event}}) + \mathrm{SfcComp}$" simulation, we retrieve a compaction rate of $0.97 \times 10^{-10}\,\mathrm{s}^{-1}$ over the 0 to 5 m depth range. This compares better with Giovinetto and Schwerdtfeger (1966) who give a compaction rate at South Pole of $5\,\mathrm{mm\,m}^{-1}\,\mathrm{a}^{-1}$, that is, roughly $1.6 \times 10^{-10}\,\mathrm{s}^{-1}$. In addition, the computed local deformation rate at 5 m depth shows an annual cycle of about $0.1 \times 10^{-10}\,\mathrm{s}^{-1}$ in amplitude around a mean of $1.3 \times 10^{-10}\,\mathrm{s}^{-1}$, the maxima being around December of each year. Although the rates above are of the same order of magnitude, the variability found between Berkner Island and South Pole may possibly be due to variations in both annual accumulation rates and mean annual air temperatures. From this we may expect the compaction rate to be even lower at Dome C indeed.

4.4 Snow temperatures

In view of the disturbances due to drifting and blowing snow at the measurement site (see Sect. 2.3), we need to identify a suitable period to evaluate the performance of the model in reproducing the snow temperatures measured within the top meter of the snow cover. The time span from 19 February 2008 to 20 March 2008 shortly after a repositioning of the upper 4 temperature sensors (see Sect. 2.3) is quite appropriate in the sense that during this period there were no important deposition and erosion events as inferred from the 13-stakes farm measurements (see Fig. 5). The upper and lower panels of Fig. 6 show comparisons of computed to measured temperatures for simulation "$\rho_{\mathrm{n, measured}}$" and the event-driven run "$\rho(U_{\mathrm{event}}) + \mathrm{SfcComp}$", respectively, each panel showing results for the snow surface temperature (T_{sfc}, upper frame) and the snow temperature at 10-cm depth ($T_{10\,\mathrm{cm}}$, lower frame).

We now first look at the simulated snow surface temperature that represents the closure of the modelled energy balance and compare it with the measured surface temperature obtained from the difference of measured upwelling and reflected downwelling longwave radiation using a snow emissivity of 0.98. It already appears from the short period shown in Fig. 6 that both runs do a very good job at reproducing the snow surface temperature even though the simulation "'$\rho(U_{\mathrm{event}}) + \mathrm{SfcComp}$" performs slightly better in terms of
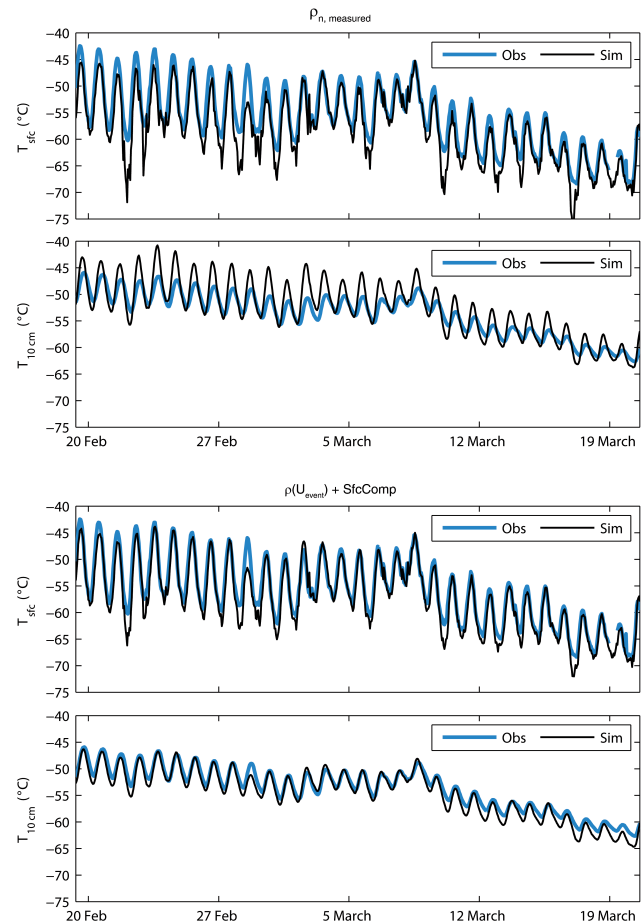

Fig. 6. Observed (Obs) and simulated (Sim) snow surface temperature T_{sfc} and snow temperature $T_{10\,\mathrm{cm}}$ at 10-cm depth, 19 February–20 March 2008. The two upper panels relate to the simulation "$\rho_{\mathrm{n, measured}}$", the two lower ones to the event-driven simulation "$\rho(U_{\mathrm{event}}) + \mathrm{SfcComp}$", that is, with additional wind densification at the surface.

temperature swings and bias. The regression of modelled to measured snow surface temperature over the time span of one month defined above corroborates this impression as for the simulation "$\rho(U_{\mathrm{event}}) + \mathrm{SfcComp}$" the slope is slightly closer to one, the intercept nearer to zero, and the mean absolute error (MAE) markedly lower (see Table 3). We attribute the difference to a marked change in simulated albedo between the two runs. Indeed, over this period, the mean parameterized albedo (see Eq. 7 and Table 1) decreases from 0.86 ± 0.02 in the "$\rho_{\mathrm{n, measured}}$" simulation to 0.83 ± 0.02 in the "$\rho(U_{\mathrm{event}}) + \mathrm{SfcComp}$" run due to differences in modelled properties at the snow surface, primarily in dendricity and sphericity. The latter value is close to the observed mean albedo of 0.81 ± 0.02, while the same run without adapting the albedo as mentioned in Sect. 3.4 yields a value of 0.86 ± 0.02 too. In other words, both simulations quite nicely reproduce the energy balance but the combination of changes

Table 3. Regression of modelled versus measured snow temperatures, slope intercept and mean absolute error (MAE), for the period 19 February to 20 March 2008, corresponding to Fig. 6. T_{sfc} is snow surface temperature and $T_{10\,\text{cm}}$ the snow temperature measured at 10-cm depth, both in °C. The simulation names are explained in Table 2.

	Simulation	slope (1)	Intercept (°C)	MAE (°C)
T_{sfc}	"$\rho_{\text{n, measured}}$"	0.98	−3.5	2.3
	"$\rho(U_{\text{event}})$ + SfcComp"	1.01	−0.6	1.4
$T_{10\,\text{cm}}$	"$\rho_{\text{n, measured}}$"	1.19	11.3	1.8
	"$\rho(U_{\text{event}})$ + SfcComp"	1.08	3.4	1.0

to the albedo parameterization and our model approach for adding snow to the underlying snow cover yields better results.

At 10-cm depth, the "$\rho(U_{\text{event}})$ + SfcComp" simulation almost perfectly matches the measurements not only with respect to the amplitude of the diurnal cycle but also regarding the timing. Note that the maxima of temperature lag about 4 h behind the maximum of incoming radiation that occurs around 01:00 p.m LT. Indeed, the model absorbs the net shortwave radiation penetrating the snowpack within the top 5 cm. This energy must then be transported by conduction deeper in the snowpack resulting in the observed lag. To the contrary, the lower density of the top layers in simulation "$\rho_{\text{n, measured}}$" allow a deeper penetration of shortwave radiation and thus the modelled temperatures at 10-cm depth show larger amplitudes compared to measurements and the maxima occur about two hours earlier than in the "$\rho(U_{\text{event}})$ + SfcComp" simulation. This comparison shows how valuable good measurements of snow temperature are as they can reveal intrinsic deficiencies of a model.

From these graphs and Table 3 we can conclude that surface and 10-cm-snow temperature are better reproduced in the "$\rho(U_{\text{event}})$ + SfcComp" simulation. But to confirm this and to show that all model adaptations were necessary, we computed for all simulations the MAE and the modified version of the coefficient of efficiency (E) of the snow temperature at 10-cm depth, the snow surface temperature, and the albedo (see Table 4). According to Legates and McCabe (1999), these two measures are less influenced by outliers than measures such as root mean squared error. We note that E ranges from minus infinity to 1, where higher values indicate a better agreement and E equal to 0 indicates that the observed mean is as good a predictor as the model.

Simulations for which the initial new snow density was obtained from measurements clearly perform worse than other simulations for all variables shown in Table 4, whereas differences are less pronounced between simulations with initial densities greater or equal to 250 kg m^{-3}. Nonetheless, especially concerning the snow temperature at 10 cm, simulations where snow was added in events perform slightly better than
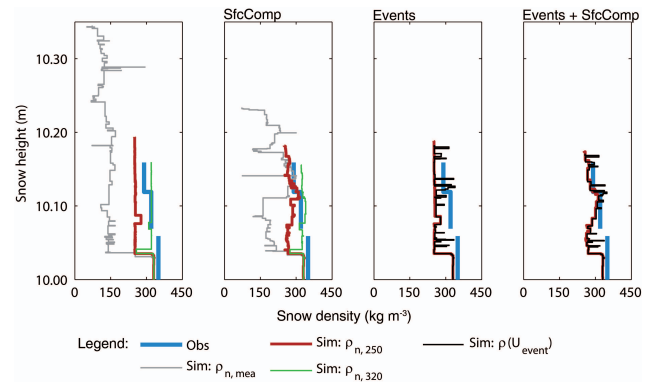

Fig. 7. Snow density profiles on 10 December 2008 as simulated with SNOWPACK using all combinations of parameterizations described in Table 2 and as observed at Concordia research station (thick, light blue line). The snow height of the observed profile is adjusted to the top of the event-driven simulation with wind compaction ("$\rho(U_{\text{event}})$ + SfcComp") but note that the density of the topmost centimetre was not recorded in the field. The leftmost panel shows simulations where the initial snow density was either measured or fixed and the snow added at the time of precipitation. The second panel from the left shows the same simulations but accounting for surface compaction due to wind through Eqs. (2) and (3). In the third panel snow density was initialized at 250 kg m^{-3} or according to Eq. (1) and snow was deposited during events. In the rightmost panel surface compaction was additionally accounted for. Colours indicate the initial snow density as described in the legend.

conventional simulations. Further analysis is required to confirm that this results from a better representation of stratification (see Sect. 4.5).

4.5 Snow profiles

A rather qualitative validation of SNOWPACK is possible by comparing observed and modelled snow stratigraphy. It is important for such a comparison that we keep in mind how they are retrieved. In the observed snow profile only layers that could somehow be detected by the observer, that is, show a sufficiently large difference in snow properties to adjacent layers, are included (Pielmeier and Schneebeli, 2003). SNOWPACK layers, however, are comparatively thin and represent a quasi-continuous snow profile, often showing no marked differences from layer to layer. In future, model outputs will have to be compared to objective measurements that match the vertical resolution of the model, revealing, for example, the small scale variability of snow density (see Brunjail et al., 2008).

In Fig. 7 we compare a snow density profile recorded at Concordia research station on 10 December 2008 to various SNOWPACK runs as described in Table 2. The date is approximately 34 months after the starting point of our main simulation period. We only show the top 15 to 35 cm of these observed and modelled profiles as below a model height of 10.05 m, the modelled snowpack originates from

Table 4. Values of mean absolute error (MAE) and modified coefficient of efficiency (E) for snow temperature at 10-cm depth (19 February 2008–20 March 2008, $n = 728$), snow surface temperature (4 May 2007–18 February 2009, $n = 13\,834$) and albedo (summer months between May 2007 and February 2009, 10 a.m.–2 p.m. LT, $n = 793$).

Name of Simulation	$T_{10\,cm}$		T_{sfc}		Albedo	
	MAE (°C)	E (1)	MAE (°C)	E (1)	MAE(1)	E (1)
$\rho_{n,\,measured}$	1.8	0.47	3.8	0.70	0.04	−2.0
$\rho_{n,\,measured}$ + SfcComp	1.5	0.56	3.6	0.71	0.04	−1.8
$\rho_{n,\,250}$	1.1	0.69	3.3	0.74	0.03	−0.9
$\rho_{n,\,250}$ + SfcComp	1.2	0.65	3.2	0.74	0.03	−0.9
$\rho_{n,\,250}$ + Event	0.9	0.73	3.2	0.74	0.02	−0.5
$\rho_{n,\,250}$ + Event + SfcComp	0.9	0.72	3.2	0.75	0.02	−0.5
$\rho_{n,\,320}$	1.1	0.68	3.2	0.75	0.02	−0.6
$\rho_{n,\,320}$ + SfcComp	1.2	0.64	3.1	0.75	0.02	−0.6
$\rho(U_{event})$	0.8	0.75	3.2	0.74	0.02	−0.5
$\rho(U_{event})$ + SfcComp	1.0	0.72	3.2	0.75	0.02	−0.5

the common initialization profile on 15 February 2008 and therefore no large differences are expected there between different model runs. The snow height of the observed profile is adjusted to the top of the event-driven simulation with wind compaction ("$\rho(U_{event})$ + SfcComp") but note that the density of the topmost centimetre was not recorded in the field. The figure reveals step by step the differences between different approaches to deal with the addition of snow to the underlying snow cover. While using the measured or estimated density of solid deposits is hardly conceivable, fixed density cannot render any stratification effects (leftmost panel). Using compaction by the wind in addition helps somewhat but the effect weakens markedly as initial density increases (second panel from the left). The next panel shows that addition of snow during events produces a pronounced stratification only if the initial density depends on the wind speed as in Eq. (1); the profile, however, remains static. Combining event based addition of snow with subsequent surface compaction results in the qualitative best agreement with this single observed profile (rightmost panel). Thus we are confident the latter two combined mechanisms have the potential to be further improved to render a realistic evolution of snow compaction at and right below the surface of the Antarctic Plateau.

In Fig. 8 we compare three snow profiles recorded at or in the vicinity of Concordia research station around 10 December 2008 to three distinctly different SNOWPACK runs "$\rho_{n,\,measured}$", "$\rho_{n,\,250}$ + SfcComp", and "$\rho(U_{event})$ + SfcComp" (all described in Table 2). The top panels show the snow density. First of all, simulation "$\rho_{n,\,measured}$", which uses the measured or estimated density of snow deposits, has a mean density much lower than that of the observed profiles. The agreement is better when in addition to overburden stress another mechanism acts to compact the solid deposits. The simulation "$\rho_{n,\,250}$ + SfcComp" therefore already has a mean density closer to the observed

profiles, but the fixed initial density of $250\,kg\,m^{-3}$ impedes the formation of higher density layers. Both the addition of snow during events using a wind speed dependent initial density and the subsequent compaction by the wind ("$\rho(U_{event})$ + SfcComp") cause a more pronounced and even denser stratification as discussed above. Note, however, that the variability of the recorded profiles does not allow for a more quantitative comparison.

The middle and lower panels of Fig. 8 show grain size and shape, respectively. Here we only compare the mean average grain size given by the observer as well as the majority grain shape (Fierz et al., 2009). There are only small differences in grain size between the two simulations, including surface compaction by the wind. They compare qualitatively well with the observed grain size profiles given the variability of the latter. The field records also show a large variability regarding grain shape. Nevertheless, all three observed profiles contain rather small, partly rounded, partly faceted grains in the top layers. Note however, that we do not model instantaneous erosion and deposition at the surface (drifting and blowing snow). Thus we cannot expect to find a much closer match between observation and simulation. At Concordia research station (light blue), the observer did find a layer of larger grains below the top layers of smaller rounded and faceted grains but classified the grains as FC (DH) or □ (∧), that is, faceted crystals with a few depth hoar crystals. Such a layer was also recorded in other places. It is questionable, however, whether this layer can be matched to the layer of large depth hoar crystals found in the simulations as this model layer was originally surface hoar buried by a subsequent snowfall in March 2007. Later on the model turned this surface hoar to the depth hoar seen in the three simulation runs. Except for the rather high modelled density of about $290\,kg\,m^{-3}$, this process is quite similar to the one Alley (1988) describes to account for low density depositional – or surface hoar – layers in polar firn.
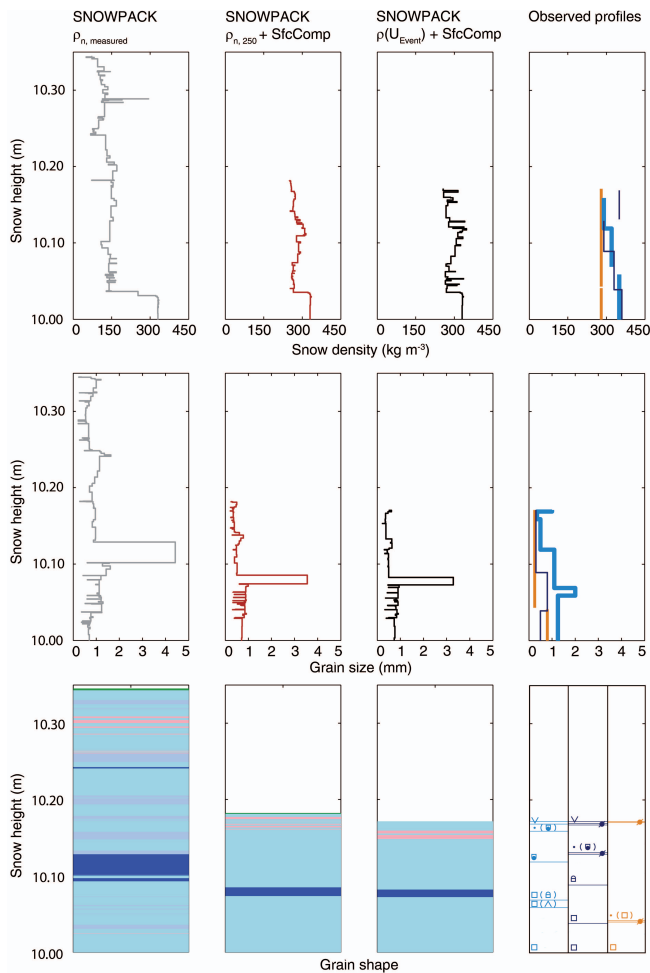
Fig. 8. Snow profile on 10 December 2008 as simulated with SNOWPACK using, from left to right, either measured new snow density as input ("$\rho_{\mathrm{n,\,measured}}$"), or an initial snow density of $250\,\mathrm{kg\,m^{-3}}$ ("$\rho_{\mathrm{n,\,250}}$ + SfcComp"), or the event-driven mechanism ("$\rho(U_{\mathrm{event}})$ + SfcComp"), the latter two with additional surface compaction due to wind. For comparison, three observed snow profiles taken in the vicinity of Concordia research station around this date are shown in the rightmost column. Note that the colours correspond to those used in Fig. 7. The observation in light blue was thus done at Concordia research station close to the sites from which observations were taken as initialization to SNOWPACK. The other observations were done at two locations 6 and 7 km NW from the research station (dark blue and orange, respectively). The snow height of the observed profile is adjusted to the top of the event-driven simulation with surface compaction ("$\rho(U_{\mathrm{event}})$ + SfcComp") but note that the density of the topmost centimetre was not recorded in the field. Top panels show snow density ($\mathrm{kg\,m^{-3}}$), middle panels grain size (mm), and bottom panels colour coded grain shapes: precipitation particles PP = lime, rounded grains RG = light pink, faceted crystals FC = light blue, depth hoar = blue, surface hoar SH = fuchsia. Additionally, rounding faceted particles FCxr are described by a mixture of light blue and light pink. Symbols represent the observed grain shapes. Both colour code and symbols follow Fierz et al. (2009).

5 Conclusions

Over a three year period, the surface snow was intensively studied at Dome C. We put a large effort in assembling a high quality data set containing information about the snow cover as well as meteorological data from automatic weather stations.

One focus of our work was the daily observation of depth, density, and water equivalent of solid deposits on tables 1 m above the snow surface. The density of these deposits could be measured over 200 times during this period of 3 yr with a mean value of $83 \pm 43\,\mathrm{kg\,m^{-3}}$. This is much lower than the density of the top 10 cm of surface snow that, from our measurements during this period, averaged to $357 \pm 14\,\mathrm{kg\,m^{-3}}$.

Comparison of these deposits to daily measurements of snow heights on two snow boards placed side by side on the surface further confirmed that the measurements on the tables 1 m above the surface are not representative of the change in snow height. We attribute the main cause of this mismatch to drifting snow that does not affect the snow surface and the deposits on the tables alike. The surface is strongly influenced by the wind as erosion and deposition occur frequently while the wind may blow away part of the shallow solid deposits on the table. This mainly affects the timing of deposition, which is continuous on the table, but very irregular on the surface. Nevertheless, because measurements are available throughout our modelling period, we used the measured or estimated mass of the deposits as precipitation input to SNOWPACK. That way we may miss over 50 % of deposited mass during shorter time periods while the mismatch reduces to about 33 % over the full simulation period.

Another aim of the present study was to model the snow-cover evolution at Dome C with SNOWPACK. That first required making SNOWPACK suitable for the Antarctic region. In particular, a new temperature dependence of snow viscosity has been introduced. We further defined a mechanism by which snow is not added at the time of precipitation but only during periods of strong winds lasting for 100 h. With this event-driven deposition, the model is suitable for long-term studies of either the snow cover or the surface mass balance in regions such as the Antarctic Plateau. For example, snow height measured at stake farms is better represented by event-driven model runs than by a simulation where new snow is added at the time of precipitation. However, when looking at shorter timescales, erosion and deposition events are of major importance. These processes are currently not implemented in the model and therefore model results may not always be accurate on short term runs.

Anyway, a much better characterization of drifting snow events is required to improve our knowledge about the processes leading to the final inclusion of new amounts of snow in the snow cover. We anticipate that future work on improving the parameterizations discussed in Sects. 3.1 and 3.2 could lead to an even more realistic modelling of observed wind crusts and maybe even glazed surfaces.

Comparing modelled and measured snow temperatures also allow the performance of the model to be tested. We showed that SNOWPACK accurately reproduces the measured snow surface temperature, that is, the energy balance is correctly computed. Furthermore, modelled snow temperatures at 10-cm depth agree very well with measurements regarding both the amplitude and the phase of temperature swings. The modified coefficient of efficiency was highest for snow temperatures at 10-cm depth in simulations with event-driven deposition. The periods over which such comparisons could be done are limited though, mostly because of either drifting and blowing snow events or missing measured data.

Finally, even though only a very qualitative comparison can be done, the top 30 to 40 cm of the simulated snow profiles show the trends observed in manually recorded profiles in terms of density, grain size, and grain shape. Here too the event-driven simulations show promising results.

Summing up, the comprehensive study presented in this paper not only produced a unique data set but also allowed for testing event-driven deposition as an input to snow-cover modelling. This deposition mechanism is based on the assumption that snow is only permanently added to the snowpack during long-lasting drifting and blowing snow events, revealing the subtle balance existing between erosion, deposition, and permanent incorporation into the snowpack. Clearly, it should be seen as an approach to snow cover modelling, rather than a true understanding of snow deposition on the Antarctic Plateau. The scheme is flexible enough to be developed further as our knowledge of the processes involved increases. Especially parameterisations of the initial snow density can be improved through additional measurements. Future research is required to investigate the influence of the new deposition mechanism on longer timescales. It remains to be shown whether total accumulation on ice sheets can be better understood when considering event-driven deposition.

References

Alley, R. B.: Concerning the deposition and diagenesis of strata in polar firn, J. Glaciol., 34, 283–290, 1988.

Arthern, R. J., Vaughan, D. G., Rankin, A. M., Mulvaney, R., and Thomas, E. R.: In situ measurements of Antarctic snow compaction compared with predictions of models, J. Geophys. Res., 115, F03011, doi:10.1029/2009jf001306, 2010.

Birnbaum, G., Freitag, J., Brauner, R., Konig-Langlo, G., Schulz, E., Kipfstuhl, S., Oerter, H., Reijmer, C. H., Schlosser, E., Faria, S. H., Ries, H., Loose, B., Herber, A., Duda, M. G., Powers, J. G., Manning, K. W., and van den Broeke, M. R.: Strong-wind events and their influence on the formation of snow dunes: observations from Kohnen station, Dronning Maud Land, Antarctica, J. Glaciol., 56, 891–902, doi:10.3189/002214310794457272, 2010.

Bromwich, D. H.: Snowfall in High Southern Latitudes, Rev. Geophys., 26, 149–168, 1988.

Brun, E., Martin, E., and Spiridonov, V.: Coupling a multi-layered snow model with a GCM, Ann. Glaciol., 25, 66–72, 1997.

Brun, E., Six, D., Picard, G., Vionnet, V., Arnaud, L., Bazile, E., Boone, A., Bouchard, A., Genthon, C., Guidard, V., Le Moigne, P., Rabier, F., and Seity, Y.: Snow/atmosphere coupled simulation at Dome C, Antarctica, J. Glaciol., 52, 721–736, 2011.

Brunjail, H., Arnaud, L., Schneebeli, M., Barnola, J.-M., and Duval, P.: Snow microstructure measurements at Concordia (East Antarctica), Workshop on the Microstructure and Properties of Firn, available at: http://engineering.dartmouth.edu/firn/posters.html, (last access: 23 December 2012), Hanover, 10–11 March 2008.

Clifton, A., Rüedi, J.-D., and Lehning, M.: Snow saltation threshold measurements in a drifting-snow wind tunnel, J. Glaciol., 52, 585–596, 2006.

Cullather, R. I., Bromwich, D. H., and Van Woert, M. L.: Spatial and Temporal Variability of Antarctic Precipitation from Atmospheric Methods, J. Climate, 11, 334–367, doi:10.1175/1520-0442(1998)011<0334:SATVOA>2.0.CO;2, 1998.

Dang, H., Genthon, C., and Martin, E.: Numerical modeling of snow cover over polar ice sheets, Ann. Glaciol., 25, 170–176, 1997.

Doumani, G. A.: Surface structures in snow, Physics of Snow and Ice, Sapporo, 1967.

Fierz, C. and Lehning, M.: Assessment of the microstructure-based snow-cover model SNOWPACK: thermal and mechanical properties, Cold Reg. Sci. Technol., 33, 123–131, doi:10.1016/S0165-232X(01)00033-7, 2001.

Fierz, C., Armstrong, R. L., Durand, Y., Etchevers, P., Greene, E., McClung, D. M., Nishimura, K., Satyawali, P. K., and Sokratov, S. A.: The International Classification for Seasonal Snow on

the Ground, IHP-VII Technical Documents in Hydrology N° 83, IACS Contribution N° 1, UNESCO-IHP, Paris, viii, 80 pp., 2009.

Frezzotti, M., Pourchet, M., Flora, O., Gandolfi, S., Gay, M., Urbini, S., Vincent, C., Becagli, S., Gragnani, R., Proposito, M., Severi, M., Traversi, R., Udisti, R., and Fily, M.: Spatial and temporal variability of snow accumulation in East Antarctica from traverse data, J. Glaciol., 51, 113–124, doi:10.3189/172756505781829502, 2005.

Frezzotti, M., Urbini, S., Proposito, M., Scarchilli, C., and Gandolfi, S.: Spatial and temporal variability of surface mass balance near Talos Dome, East Antarctica, J. Geophys. Res.-Earth, 112, F02032, doi:10.1029/2006jf000638, 2007.

Fujiwara, K. and Endo, Y.: Preliminary report of glaciological studies, Polar Research Centre, National Science Museum, Tokyo, 68–109, 1971.

Gallée, H., Guyomarc'h, G., and Brun, E.: Impact of snow drift on the antarctic ice sheet surface mass balance: Possible sensitivity to snow-surface properties, Bound.-Lay. Meteorol., 99, 1–19, 2001.

Gay, M., Fily, M., Genthon, C., Frezzotti, M., Oerter, H., and Winther, J. G.: Snow grain-size measurements in Antarctica, J. Glaciol., 48, 527–535, 2002.

Genthon, C., Town, M. S., Six, D., Favier, V., Argentini, S., and Pellegrini, A.: Meteorological atmospheric boundary layer measurements and ECMWF analyses during summer at Dome C, Antarctica, J. Geophys. Res.-Atmos., 115, D05104, doi:10.1029/2009jd012741, 2010.

Giovinetto, M. B. and Schwerdtfeger, W.: Analysis of a 200 year snow accumulation series from the South Pole, Meteorol. Atmos. Phys., 115, 227–250, doi:10.1007/BF02246754, 1966.

Goodwin, I. D.: Snow accumulation and surface topography in the katabatic zone of Eastern Wilkes Land, Antarctica, Antarct. Sci., 2, 235–242, 1990.

King, J. C. and Turner, J.: Antarctic Meteorology and Climatology, Cambridge University Press, Cambridge, 409 pp., 1997.

Kotlyakov, V. M.: The snow cover of the Antarctic and its role in the present-day glaciation of the continent, Results of the investigation in the IGY glaciological programm, section 9, number 7, IPST, Jerusalem, 256 pp., 1966.

Lanconelli, C., Busetto, M., Dutton, E. G., König-Langlo, G., Maturilli, M., Sieger, R., Vitale, V., and Yamanouchi, T.: Polar baseline surface radiation measurements during the International Polar Year 2007–2009, Earth Syst. Sci. Data, 3, 1–8, doi:10.5194/essd-3-1-2011, 2011.

Legates, D. R., and McCabe, G. J.: Evaluating the use of "Goodness-of-fit" Measures in hydrologic and hydroclimatic model validation, Water Resour. Res., 35, 233–241, doi:10.1029/1998wr900018, 1999.

Lehning, M. and Fierz, C.: Assessment of snow transport in avalanche terrain, Cold Reg. Sci. Technol., 51, 240–252, 2008.

Lehning, M., Bartelt, P., Brown, B., Fierz, C., and Satyawali, P.: A physical SNOWPACK model for the Swiss avalanche warning Part II: Snow microstructure, Cold Reg. Sci. Technol., 35, 147–167, 2002a.

Lehning, M., Bartelt, P., Brown, B., and Fierz, C.: A physical SNOWPACK model for the Swiss avalanche warning Part III: Meteorological forcing, thin layer formation and evaluation, Cold Reg. Sci. Technol., 35, 169–184, 2002b.

Mellor, M.: Blowing Snow, Cold Regions Science and Engineering Part 3, 79, 1965.

Morris, E. M., Bader, H. P., and Weilenmann, P.: Modelling temperature variations in polar snow using DAISY, J. Glaciol., 43, 180–191, 1997.

Nishimura, K. and Hunt, J. C. R.: Saltation and incipient suspension above a flat particle bed below a turbulent boundary layer, J. Fluid Mech., 417, 77–102, doi:10.1017/s0022112000001014, 2000.

Palais, J. M., Whillans, I. M., and Bull, C.: Snow stratigraphic studies at Dome C, East Antarctic: An investigation of depositional and diagenetic processes, Ann. Glaciol., 3, 239–242, 1982.

Petit, J. R., Jouzel, J., Pourchet, M., and Merlivat, L.: A detailed study of snow accumulation and stable isotope content in Dome C (Antarctica), J. Geophys. Res.-Oc. Atm., 87, 4301–4308, 1982.

Pielmeier, C. and Schneebeli, M.: Developments in snow stratigraphy, Surv. Geophys., 24, 389–416, 2003.

Pomeroy, J. W. and Gray, D. M.: Snowcover: Accumulation, Relocation and Management., National Hydrology Research Institute, Saskatoon, Canada, 144 pp., 1995.

Pomeroy, J. W., Gray, D. M., and Landine, P. G.: The Prairie Blowing Snow Model: characteristics, validation, operation, J. Hydrol., 144, 165–192, 1993.

Radok, U. and Lile, R. C.: A year of snow accumulation at Plateau Station, in: Meteorological Studies at Plateau Station, Antarctica, in: Antar. Res. Ser., edited by: Businger, J. A., American Geophysical Union, Washington DC, 17–26, 1977.

Sato, T., Kosugi, K., Mochizuki, S., and Nemoto, M.: Wind speed dependences of fracture and accumulation of snowflakes on snow surface, Cold Reg. Sci. Tech., 51, 229–239, 2008.

Schweizer, J., Michot, G., and Kirchner, H. O. K.: On the fracture toughness of snow, Ann. Glaciol., 38, 1–8, doi:10.3189/172756404781814906, 2004.

Seligman, G.: Snow Structure and Ski Fields, MacMillan and Co., London, 555 pp., 1936.

Stearns, C. R. and Weidner, G. A.: Sensible and latent heat flux estimates in Antarctica, in: Antarctic meteorology and climatology, studies based on automatic weather stations, in: Antar. Res. Ser., edited by: Bromwich, D. H. and Stearns, C. R., AGU, Washington D.C., 61, 109–138, 1993.

Sugiyama, S., Enomoto, H., Fujita, S., Fukui, K., Nakazawa, F., Holmlund, P., and Surdyk, S.: Snow density along the route traversed by the Japanese–Swedish Antarctic Expedition 2007/08, J. Glaciol., 58, 529–539, doi:10.3189/2012JoG11J201, 2012.

Vionnet, V., Brun, E., Morin, S., Boone, A., Faroux, S., Le Moigne, P., Martin, E., and Willemet, J.-M.: The detailed snowpack scheme Crocus and its implementation in SURFEX v7.2, Geosci. Model Dev., 5, 773–791, doi:10.5194/gmd-5-773-2012, 2012.

Walden, V. P., Warren, S. G., and Tuttle, E.: Atmospheric ice crystals over the Antarctic Plateau in winter, J. Appl. Meteorol., 42, 1391–1405, 2003.

Watanabe, O.: Distribution of Surface Features of Snow Cover in Mizuho Plateau, Memoirs of National Institute of Polar Research, 7, 154–181, 1978.